Coordination Chemistry Reviews 254 (2010) 2634–2642

Contents lists available at ScienceDirect

Coordination Chemistry Reviews

journal homepage: www.elsevier.com/locate/ccr

Review

Mechanisms of sensitization of lanthanide(III)-based luminescence in transition metal/lanthanide and anthracene/lanthanide dyads

Michael D. Ward*

Department of Chemistry, University of Sheffield, Sheffield S3 7HF, UK

Contents

ARTICLE INFO

Article history:
Received 11 September 2009
Accepted 1 December 2009
Available online 5 December 2009

Keywords:
Luminescence
Energy-transfer
Lanthanide
Ruthenium
Osmium
Chromium
Cobalt
Anthracene

ABSTRACT

Four sets of dyads are discussed, in all of which near-infrared emitting lanthanide(III) ions such as Nd(III), Er(III) or Yb(III) are energy-acceptors which provide sensitized luminescence following energy-transfer from an antenna group. In three sets of dyads the antenna (energy-donor) group is a luminescent transition metal fragment; in the fourth the antenna is an anthracene group. A combination of photophysical studies and calculations has been used to understand the mechanisms by which energy-transfer to the lanthanide(III) ion occurs. Although definitive answers are not possible in every case due to the presence of several possible energy-transfer pathways, the relative contributions of Förster-type, Dexter-type and redox-mediated energy-transfer pathways have been analysed. Interesting results include (i) the demonstration of pure Dexter energy-transfer over 20 Å in a Ru(II)/Nd(III) dyad, and (ii) the demonstration of a redox-based mechanism for energy-transfer in anthracene/Ln(III) dyads in which the first step is photoinduced *electron*-transfer from the excited anthracene chromophore to a diimine ligand on the lanthanide(III) to generate a charge-separated state.

1. Introduction

1.1. Background

Lanthanide-based luminescence is usually sensitized by energy-transfer (hereafter abbreviated as EnT, since 'ET' is commonly used for 'electron-transfer') from a nearly strongly absorbing chromophoric antenna group in order to overcome the main problem with direct excitation, which is that the f–f transitions of lanthanide ions are Laporte forbidden and very weak [1]. Usually a ligand containing an aromatic ring acts as the light-absorbing fragment, and this will have a high extinction coefficient for absorption in the UV region. The widely accepted mechanism which usually operates is that excitation into the (fully allowed) singlet excited state of the ligand is followed by fast inter-system crossing to generate a ligand-based triplet state, and it is this triplet state that transfers its energy to the Ln(III) centre to generate a luminescent f–f state *via* a Dexter double electron-exchange mechanism which is made possible by direct contact between aromatic ligand and Ln(III) ion, thereby providing the electronic coupling and short distance which facilitate the Dexter EnT process (see next section). There is a huge amount of evidence to support this picture [1].

This mechanism does not always operate however. Sometimes, for example, EnT to the Ln(III) centre can occur directly from the singlet excited state of the ligand [2]. In some other cases a

* Department of Chemistry, University of Sheffield, Dainton Building, Brook Hill, Sheffield S3 7HF, UK. Tel.: +44 114 2229484; fax: +44 114 2229346.
E-mail address: m.d.ward@Sheffield.ac.uk.

0010-8545/$ – see front matter © 2009 Elsevier B.V. All rights reserved.
doi:10.1016/j.ccr.2009.12.001

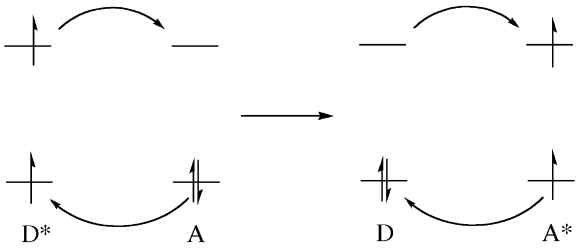

Scheme 1. Dexter energy-transfer by the double electron-exchange mechanism, allowing the triplet excited state of the donor (D*) to transfer its energy to the acceptor (A) which likewise ends up in the triplet excited state A*.

redox-based mechanism operates in which the first step is actually photoinduced *electron*-transfer to the Ln(III) ion, which is possible for Eu(III) and Yb(III) since both of these have readily accessible Ln(II) states [3]. In this case, back electron-transfer to the ground state liberates enough energy to leave the Ln(III) ion in its emissive f–f excited state (Scheme 2; see next section).

In recent years the variety of antenna groups used to sensitize Ln(III)-based luminescence has increased substantially, and in particular transition metal chromophores have been used as energy-donors in d–f hybrid complexes in which excitation of the d-block unit, often into a long-lived MLCT state, is followed by d → f EnT [4]. This allows, for example, relatively long wavelength light in the visible region to be used to generate sensitized near-IR luminescence from low-energy emitting Ln(III) ions such as Yb(III), Nd(III), Er(III) and Pr(III). The use of transition metal species as sensitizers for Ln(III)-based emission in d–f hybrids has recently been reviewed [4]. In many cases the mechanism by which the d-block energy-donor transits its energy to the f-block energy-acceptor is not obvious and has not been explicitly considered; the fact that absorption of light by the transition metal antenna group is followed by emission of light from the Ln(III) centre is sufficient for the purposes of the papers. It is obvious in many such cases that the d → f EnT is slow and inefficient, a consequence of the high inter-chromophore separation and the presence in some cases of saturated bridging ligands.

We have been interested recently in investigating the mechanism of EnT to Ln(III) ions in a range of systems in which the 'standard' mechanism depicted in Scheme 1 may not apply. This includes many d/f complexes, and also a complex based on anthracene as a sensitizing antenna group. In this short review we summarise the results of four recent studies in which the mechanism of EnT from a chromophore to the Ln(III) centre has been explicitly considered and analysed by a combination of time-resolved photophysical methods and calculations.

1.2. Summary of EnT mechanisms

It is appropriate at this point to review briefly the principal EnT mechanisms operating in any energy-donor/acceptor pairs. These are the Förster [6] and Dexter [6] mechanisms, and the principles behind them are expressed in Eqs. (1) and (2), with the overlap integrals featuring in these equations given in Eqs. (3) and (4). In Eq. (1), κ is the factor taking account of the relative orientation of donor and acceptor dipoles (generally taken as 2/3 for a randomly oriented system); ϕ is the emission quantum yield and τ is the (unquenched) emission lifetime of the donor; n is the refractive index of the solvent; and d is the inter-chromophore distance. In Eq. (2), H is the donor/acceptor electronic coupling.

$$k_{en}{}^{F} = \frac{8.8 \times 10^{-25} \kappa^2 \phi}{n^4 \tau d_{MM}{}^{6}} J_F \quad (1)$$

$$k_{en}{}^{D} = \frac{4\pi^2 H^2}{h} J_D \quad (2)$$

$$J_F = \frac{\int D(\bar{\upsilon}) A(\bar{\upsilon}) / \bar{\upsilon}^4 d\bar{\upsilon}}{\int D(\bar{\upsilon}) d\bar{\upsilon}} \quad (3)$$

$$J_D = \frac{\int D(\bar{\upsilon}) A(\bar{\upsilon}) d\bar{\upsilon}}{\int D(\bar{\upsilon}) d\bar{\upsilon} \int A(\bar{\upsilon}) d\bar{\upsilon}} \quad (4)$$

Förster EnT (Eq. (1)) is a through-space mechanism based on a Coulombic interaction between the multipole changes associated with the excited state to ground state transition in the energy-donor, and the ground state to excited state transition in the energy-acceptor. The main component is generally considered to be the dipole–dipole interaction, which is the basis of Eqs. (1) and (2). This has a d^{-6} distance dependence because of its linear dependence on the electric field associated with both donor and acceptor transition dipole moments, each of which diminishes as d^{-3}. Its efficiency depends on the integrated overlap between the (normalized) emission spectrum of the donor, and the absorption spectrum of the donor (Eq. (3)). A spin selection rule is implicit in this: for the absorption spectrum of the acceptor to be intense, giving the necessary high spectroscopic overlap, the transitions must be spin-allowed. Global conservation of spin implies that therefore no spin change can occur at the donor either. Since the ground states of organic chromophores and fluorophores are usually spin-paired singlets, the relevant spin-allowed excited states must likewise be singlet states, and this leads to the commonly expressed approximation that Förster EnT is a 'singlet-to-singlet' process, an approximation which holds well for systems containing no heavy atoms. In favourable situations, Förster EnT can operate over distances up to *ca.* 100 Å, which makes it valuable and widely used in FRET-type assays of biological systems [7].

Higher-order multipolar contributions also contribute to Förster-type EnT, and can be of particular importance when the dipole–dipole contribution is minimal because of the low absorption coefficients of the acceptor when the transitions are dipole forbidden [as with lanthanide(III) ions]. Thus a donor/acceptor dipole/quadrupole interaction can contribute to energy-transfer in cases where the dipole/dipole mechanism is inoperative, and indeed f–f transitions may have significant transition quadrupole moments: the 'allowedness' of this can overcome the higher distance dependence (d^{-8}, compared to d^{-6} for the dipole–dipole mechanism of Eq. (1)) [8].

In contrast Dexter EnT (Eq. (2) and (4)) is a double electron-exchange mechanism whereby one electron is transferred in each direction between energy-donor and energy-acceptor components (Scheme 1) [5]. This requires through-bond electronic coupling, exactly as for single electron-transfer, and is therefore facilitated by good orbital overlap in conjugated systems. A consequence of this is that it permits EnT in situations where the Förster mechanism cannot operate because of the spin selection rules. The example shown in Scheme 1 shows a triplet excited state of an energy-donor collapsing to a singlet ground state, and the ground state of the energy-acceptor being excited to a triplet state. The Förster mechanism would be ineffective here because the necessary spin–forbidden absorption of the acceptor would (in a light-atom system) have a vanishingly small absorption coefficient, leading to no significant donor/acceptor overlap as expressed by Eq. (3). The double electron-exchange of the Dexter mechanism avoids this spin selection rule at each centre (although the spin of the whole assembly must be preserved) and consequently Dexter EnT is sometimes called 'triplet–triplet' EnT. It is emphasized that these limiting cases of 'singlet' and 'triplet' EnT cease to apply when heavy atoms are involved because of the effects of spin–orbit coupling.

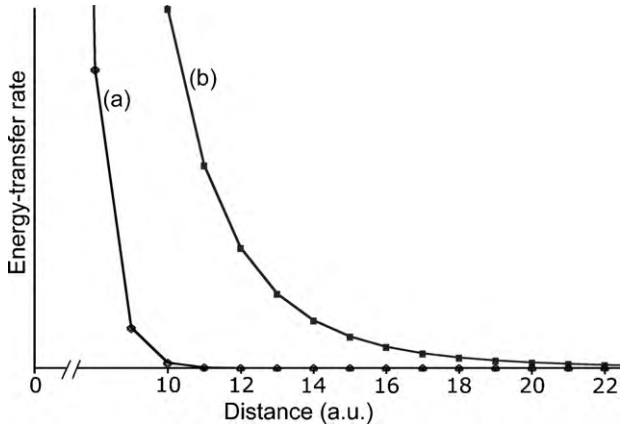

Fig. 1. Relative distance dependencies of Dexter energy-transfer [curve (a)] and Förster dipole–dipole energy-transfer [curve (b)]. Both curves start from the same point on the *y*-axis.

The occurrence of a spin–forbidden conversion at each centre is reflected in the way that the donor/acceptor spectroscopic overlap integral is calculated for Dexter EnT (Eq. (4)). Overlap between the emission spectrum of the donor and the absorption spectrum of the acceptor is still required, but *both* spectra are normalized such that the intensities are irrelevant, the intensity being related in part to the spin-allowedness of each transition and therefore no longer an issue. The overlap calculated in this way therefore becomes just a manifestation of a good energy match between start and end states, something which is desirable for any electron-transfer processes as expressed in Fermi's golden rule.

A single electron-transfer process depends on the electronic coupling H between donor and acceptor, and consequently the double electron-transfer involved in Dexter EnT depends on the square of this. Since H has an inverse exponential dependence on distance d, it follows that Dexter EnT falls off as e^{-2d}.

The different distance dependencies of Förster and Dexter EnT are shown in Fig. 1. It is clear that the function e^{-2d} decays with distance more quickly than d^{-6}, such that–all other things being equal—Förster (dipole–dipole) EnT is expected to operate over much longer distances than Dexter EnT which tails off much more quickly. In fact Dexter EnT was originally defined as involving *direct* orbital overlap between donor and acceptor [5], which cannot be maintained over more than a few Ångstroms even when diffuse and extended atomic orbitals are involved. However double electron-exchange between donor and acceptor is also generally considered as Dexter EnT even when the orbitals of an intermediate bridging ligand are involved in mediating the electron-transfers (superexchange); strictly speaking EnT in such extended systems should be denoted 'Dexter-type' rather than pure Dexter, although the distinction is not often used [9].

Finally, as mentioned briefly earlier, there is a quite different EnT mechanism available that is specific to dyads in which Eu(III) or Yb(III) are the energy-acceptor; this was first proposed by Horrocks in 1997 [3c]. These ions both have a readily accessible Ln(II) state as a consequence of the stable electron configurations $4f^7$ for Eu(II) and $4f^{14}$ for Yb(II). If the excited state of the antenna group is a good electron donor, which is often the case because an electron has been promoted to a high energy orbital, then the first step can be photoinduced *electron*-transfer from the excited donor D* to Ln(III) to generate a charge-separated $D^{\bullet+}$–Ln(II) state. This requires D* to be a sufficiently good electron donor to be able to reduce the Ln(III) ion concerned. Rapid back electron-transfer can then liberate enough energy to leave the Ln(III) ion in its luminescent excited state, *i.e.* D–Ln(III)*, depending on how much energy is liberated by the back electron-transfer. If Eu(III) is the acceptor then the back electron-transfer step needs to liberate *ca.* 17,200 cm^{-1} (2.1 eV) to pump Eu(III) to its emissive $^5D_0$ state; if less energy than this is available then the excited state of the donor will be quenched by Eu(III), but no sensitized luminescence will be seen from Eu(III) and the energy is wasted as heat. With Yb(III) as acceptor however, its lower energy luminescent f–f state means that only 10,200 cm^{-1} (1.3 eV) needs to be liberated in the back electron-transfer step to generate excited Yb(III) and result in sensitized near-infrared luminescence [3c].

Because the first step of this EnT process is a conventional electron-transfer step, it is not dependent on donor/acceptor spectroscopic overlap in the way that is required for the Förster and Dexter mechanisms. In fact the mechanism was first identified when EnT to Eu(III) and Yb(III) was observed to be anomalously fast in dyads in which there was no donor/acceptor overlap.

2. Results and discussion

2.1. Example 1: $[M(CN)_6]^{3-}$ (M = Cr, Co) as energy-donors to Yb(III) and Nd(III).

We have described several cyanide-bridged networks in which the ^{3}MLCT states of luminescent complexes such as $[M(bipy)(CN)_4]^{2-}$ (M = Ru, Os) and their derivatives act as energy-donors to near-IR emitting Ln(III) ions such as Nd(III) and Yb(III) [10]. Although we have not performed calculations on these systems the short metal–metal separations (*ca.* 5.5 Å across the M–CN–Ln bridge) and directly conjugated pathway imply that the Dexter mechanism could be operating, and we have studied this explicitly in some $[M(CN)_6]^{3-}$/Ln(III) dyad systems (M = Cr, Co) [11].

These simple hexacyanometallates of Cr(III) and Co(III) have spin–forbidden d–d excited states which result in long-lived phosphorescence in the red region of the spectrum, from $^3T_{1g} \rightarrow {}^1A_{1g}$ (for Co) and $^2E_g \rightarrow {}^4A_{2g}$ (for Cr) transitions. Although this phosphorescence is usually only observable at low temperatures, in *e.g.* simple potassium salts, the presence of a heavy metal such as a Ln(III) ion facilitates inter-system crossing from the initially populated spin-allowed d–d excited states to the lower energy spin–forbidden states and permits the phosphorescence to be seen at room temperature [12].

Slow evaporation of solutions containing a 1:1 mixture of $K_3[M(CN)_6]$ and a $Ln(NO_3)_3$ in aqueous dmf afforded the cyanide-bridged dinuclear complexes $[Ln(dmf)_4(H_2O)_3(\mu\text{-}CN)Co(CN)_5]\cdot nH_2O$ (abbreviated Co–Ln; Ln = Gd, Nd, Yb) and the one-dimensional polymeric chains $\{[Cr(CN)_4(\mu\text{-}CN)_2Ln(H_2O)_2(dmf)_4]\cdot nH_2O\}_\infty$ (abbreviated Cr–Ln; Ln = Gd, Nd, Yb). The former series contains discrete dinuclear units in which the $[Co(CN)_6]^{3-}$ anion is connected to a $\{Ln(dmf)_4(H_2O)_3\}^{3+}$ cation *via* a single cyanide bridge, making the Ln(III) centre 8-coordinate. The Cr/Ln complexes in contrast are infinite one-dimensional ...Ln–NC–Cr–CN–Ln... chains in which $\{Ln(dmf)_4(H_2O)_2\}^{3+}$ and $[Cr(CN)_6]^{3-}$ anions alternate, with a *cis*-related pair of cyanides from each $[Cr(CN)_6]^{3-}$ anion involved in bridging. An example is shown in Fig. 2; the Cr···Yb separations are 5.59 and 5.58 Å.

The solid-state absorption spectra of the two series show a combination of the spin-allowed d–d transitions associated with the $[M(CN)_6]^{3-}$ anions in the UV region, plus sharper and weaker peaks in the visible and near-IR regions associated with the Ln(III) f–f absorptions. When Ln = Gd there are no f–f absorptions apparent as the lowest such transition for Gd(III) lies in the UV region and is obscured by the more intense d–d transitions. For Ln = Yb there is a single f–f absorption at *ca.* 980 nm, associated with the sole excited state of Yb(III); for Nd(III) in contrast there are numerous sharp, weak f–f absorption bands in the visible region.

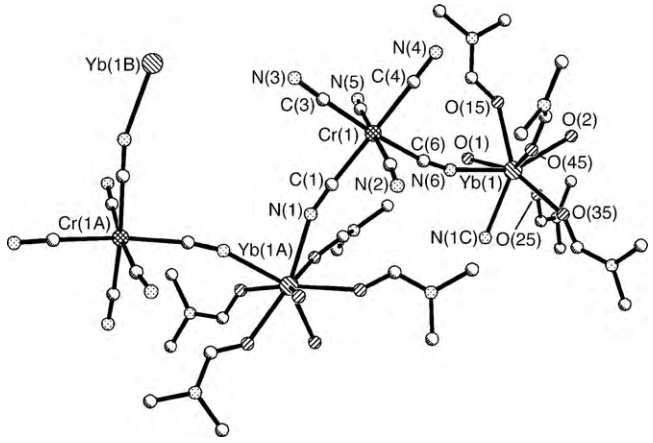

Fig. 2. Part of the structure of the one-dimensional zig-zag chain compound $\{[Cr(CN)_6][Yb(dmf)_4(H_2O)_2]\cdot H_2O\}_\infty$ (from Ref. [11]).

The luminescence properties of Co–Gd and Cr–Gd were studied as controls, because in these cases Co–Gd and Cr–Gd EnT cannot occur [the lowest f–f level of Gd(III) is at >30,000 cm^{-1}], so these two complexes will display the unquenched luminescence of the hexacyanometallate units. Excitation of Co–Gd into the d–d absorption bands at 380 nm resulted in appearance of a broad phosphorescence at 700 nm from the Co-centred $^3T_{1g} \rightarrow {}^1A_{1g}$ transition, with a lifetime of 630 ns. Similarly, excitation of Cr–Gd afforded emission at 820 nm from the Cr-centred $^2E_g \rightarrow {}^4A_{2g}$ transition, with a lifetime of 1.3 μs (Fig. 3).

The complexes Co–Ln (Ln = Nd, Yb) and Cr–Ln (Ln = Nd, Yb) behaved quite differently on excitation into the d–d absorptions. In every case the phosphorescent emission from the d-block unit was completely absent, undetectable with the experimental setup used, and instead sensitized Nd-based or Yb-based emission was observed at the characteristic wavelengths [11,400, 9400 and 7500 cm^{-1} for the $^4F_{3/2} \rightarrow {}^4I_{9/2}$, $^4F_{3/2} \rightarrow {}^4I_{11/2}$ and $^4F_{3/2} \rightarrow {}^4I_{13/2}$ transitions of Nd(III); and 10,200 cm^{-1} for the $^2F_{5/2} \rightarrow {}^2F_{7/2}$ transition of Yb(III)]. Assuming that we could detect residual d-block phosphorescence with a lower lifetime limit of 10 ns, the absence of such emission implies a d → f EnT rate of $\geq 10^8\ s^{-1}$. In agreement with this, time-resolved measurements on the Ln(III)-based emission showed in every case no rise-time, *i.e.* any rise-time is shorter than 10 ns.

The question now arises as to the mechanism of EnT. Fig. 3 shows the superposition of the donor (d-block unit) emission spectra with the acceptor [Nd(III) or Yb(III)] absorption spectra. It is obvious that the emission spectra of both the $[M(CN)_6]^{3-}$ units (M = Co, Cr) overlap with several of the Nd(III) f–f absorptions; there is also overlap, albeit clearly much less, between the tails of the d-block emission bands and the sole Yb(III)-based f–f absorption. For the Co–Ln pair (Ln = Nd, Yb) we used the available spectral data to calculate the Förster (dipole–dipole) and Dexter overlap integrals as expressed in Eqs. (3) and (4). For Co → Nd EnT, the calculated Förster overlap J_F of $6.4 \times 10^{-17}\ cm^3\ M^{-1}$ means that the critical transfer distance R_C, beyond which EnT becomes less than 50% efficient, is 7.8 Å, and the rate of Förster EnT (given the distance of *ca.* 5.6 Å from crystallographic data) would be $1.6 \times 10^7\ s^{-1}$. An EnT rate this slow would leave significant residual Co(III)-based phosphorescence with a lifetime of around 60 ns—which was not observed. Thus we can rule out the dipole–dipole mechanism here on the basis of an observed EnT rate of at least $10^8\ s^{-1}$.

The possibility of a dipole–quadrupole contribution exists however (this was not considered in the original paper [11]), although we cannot calculate this explicitly as we do not know the oscillator strength of the quadrupole f–f transition. We note however

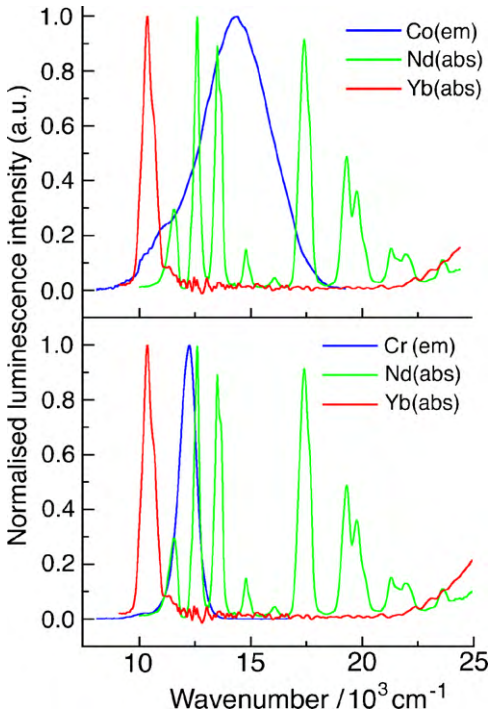

Fig. 3. Overlap of the d-block emission spectra {of the $[M(CN)_6]^{3-}$ unit: M = Co (top) or Cr (bottom)} with the absorption spectra of Nd(III) and Yb(III) ions in the Ln(III)/hexacyanometallate salts described in Ref. [11].

that in related cases in which the energy-acceptor has very weak dipole–forbidden electronic transitions, the dipole–quadrupole contribution to multipolar EnT can operate over a greater distance than the dipole–dipole contribution [8].

The Dexter overlap integral J_D of 1.1×10^{-4} cm means that Co → Nd EnT could also occur by the Dexter mechanism over this distance, with a rate of $10^8\ s^{-1}$, provided only that the electronic coupling *H* has a value of *ca.* 1 cm^{-1}. This is a modest value which is readily achievable by interaction of the metal orbitals with the bridging cyanide, even allowing for the very small covalency associated with 4f orbitals. For the complex Co–Nd the complete quenching of Co(III)-based emission by fast EnT to Nd(III) could accordingly occur *via* the Dexter mechanism.

In Co–Yb both J_F and J_D are smaller, at $5.2 \times 10^{-18}\ cm^3\ M^{-1}$ and 5.4×10^{-4} cm, respectively. The reduced J_F value compared to Co–Nd means that the critical transfer distance is also smaller, and is calculated to be 5.2 Å, rather smaller than the actual Co···Yb separation; over a distance of 5.6 Å, dipole–dipole EnT would be less than 50% efficient and occur with a rate of only $1.3 \times 10^6\ s^{-1}$, leaving a substantial and easily detected residue of Co(III)-based phosphorescence (which was not present). Again however the possibility exists of a dipole–quadrupole contribution [8]. If we assume Dexter EnT, it is only necessary for the electronic coupling *H* to exceed *ca.* 1.5 cm^{-1} for the rate of Co → Yb EnT to exceed $10^8\ s^{-1}$.

In these Co–Ln systems therefore the calculations quite clearly rule out a dipole–dipole contribution to the Co → Ln EnT. The observed EnT could occur *via* the Dexter mechanism, a consequence of the short distance and the electronic coupling between the metal centres mediated by the cyanide ligand [11]; or *via* a dipole/quadrupole Förster-type mechanism.

2.2. Example 2: long-range Dexter EnT from $[Ru(bipy)_3]^{2+}$ as donor unit

In this next set of compounds (Schemes 2 and 3), we were interested to examine EnT over much greater distances, and to

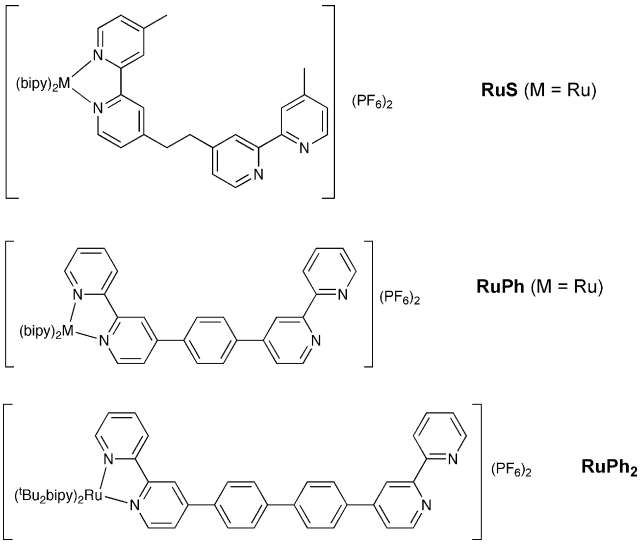

Scheme 2. Ru(II) complexes used to make Ru(II)/Ln(III) dyads as shown in Scheme 3 (from Ref. [13]).

compare saturated and unsaturated bridging ligands. $[Ru(bipy)_3]^{2+}$ is of course a very well-known fluorophore and has been used as energy-donors to Yb(III) and Nd(III) in a few d/f dyads [4]. However in most cases the EnT is slow and inefficient and the mechanism not discussed.

We prepared the series of complexes shown in Scheme 2 in which a $[Ru(bipy)_3]^{2+}$ derivative is connected to an additional vacant bipyridyl binding site *via* a spacer with is either saturated (ethylene) or conjugated (*p*-phenylene, *p*-biphenylene) [13]. Reaction of these with excess $[Ln(tta)_3(H_2O)_2]$ in CH_2Cl_2 solution affords dinuclear d–f hybrids *via* an equilibrium reaction of the type shown in Scheme 3, in which the vacant bipyridyl site of the d-block 'complex ligand' displaces two water ligands from the coordination sphere of the Ln^{III} species to give an eight-coordinate $\{Ln(tta)_3(bipy)\}$ centre with a high association constant (*ca.* 10^7 M^{-1}) in CH_2Cl_2.

We performed a series of spectroscopic titrations in which portions of $[Ln(tta)_3(H_2O)_2]$ (Ln = Nd, Er, Yb) were titrated into a solution of the relevant Ru(II) complex in CH_2Cl_2. Although we used several lanthanide species the most clear-cut results were obtained using Nd(III), which is the most effective energy-acceptor in these systems due to a high density of f–f states in the region overlapping with the Ru(II)-based emission, and so we focus here

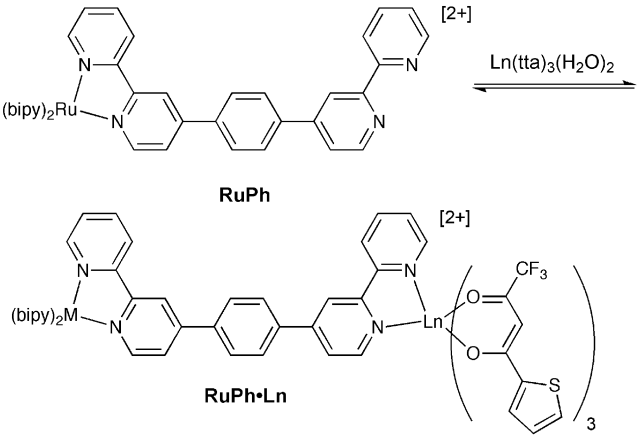

Scheme 3. Preparation of Ru(II)/Ln(III) dyads form the 'complex ligands' shown in Scheme 2 (from Ref. [13]).

on the behaviour of the three Ru–Nd dyads. As each Ru–Nd dyad formed, the occurrence of Ru → Nd EnT within the dyad could be monitored in two ways. Firstly, the luminescence intensity of the Ru(II) centre was progressively quenched, and time-resolved measurements revealed the onset of a short-lived luminescence component which became dominant as the titration progressed and the free Ru(II) complex (long-lived luminescence) was replaced by the Ru–Nd dyad (short-lived luminescence). In the case of RuPh, for example, the 520 ns Ru-based luminescence components was steadily replaced by a shorter-lived (48 ns) component as the dyad RuPh·Nd formed. From this, and using Eq. (5), it is simple to calculate the Ru → Nd EnT rate k_{EnT} as 1.9×10^7 s^{-1} (in Eq. (5), τ_u is the 'unquenched' emission lifetime of the donor chromophore; and τ_q is the lifetime of the luminescence that has been partially quenched by energy-transfer).

$$k_{EnT} = \tau_q^{-1} - \tau_u^{-1} \quad (5)$$

Secondly, the occurrence of Ru → Nd EnT could be demonstrated by monitoring the sensitized luminescence from Nd(III) when excitation was selective into the ^{3}MLCT band of the Ru(II) centre at 460 nm, such that no direct excitation of Nd(III) could occur. The near-IR emission from Nd(III) can only have arisen from Ru → Nd EnT, a fact which is confirmed by the presence of a grow-in with a time constant of *ca.* 60 ns, a good match for the 48 ns decay of the partially quenched Ru(II) centre.

To help decide on the EnT mechanism we calculated the Förster and Dexter overlap integrals. The J_F value of 6.3×10^{-17} cm^3 M^{-1} results in a critical transfer distance of 8.5 Å for Förster EnT, which rules out the Förster (dipole–dipole) mechanism completely given a Ru···Nd separation of *ca.* 15.6 Å, although a higher order dipole/quadrupole contribution cannot be ruled out at this stage. The Dexter overlap integral J_D of 1.6×10^{-4} cm means that Ru → Nd EnT could occur at the observed rate of 1.9×10^7 s^{-1} as long as the electronic coupling H is at least 0.3 cm^{-1}, a low value which is quite feasible given the conjugated bridging ligand.

Comparison of the properties of RuPh·Nd with those of RuS·Nd and $RuPh_2$·Nd rule out Förster EnT and confirm that the Dexter mechanism is operating in RuPh·Nd. In RuS·Nd, with a saturated spacer, the degree of quenching of Ru(II) emission by the Nd(III) centre is much less: the emission lifetime drops from 390 to 210 ns giving a smaller k_{EnT} value of 2.2×10^6 s^{-1} (Eq. (5)) Thus the EnT is an order of magnitude slower in RuS·Nd than in RuPh·Nd despite the shorter metal–metal separation (molecular mechanics calculations show that the Ru···Nd separation can lie in the range 9.6–13.4 Å), which can only be explained if the EnT occurs *via* the conjugated bridging ligand in RuPh·Nd, *i.e.* Dexter EnT is operative. The occurrence of any Ru → Nd EnT at all in RuS·Nd can be ascribed to its conformational flexibility; in the most folded conformation the Ru···Nd separation of 9.6 Å is not much greater than the Förster critical transfer distance of 8.3 Å, allowing a small amount of EnT *via* the dipole–dipole mechanism and possibly some also by a dipole/quadrupole mechanism.

In $RuPh_2$·Nd greater Ru···Nd separation across the longer bridging ligand naturally slows the EnT rate: the reduction in Ru(II)-based emission lifetime from 460 ns in $RuPh_2$ to 256 ns in $RuPh_2$·Nd results in an EnT rate of 1.7×10^6 s^{-1}. The slower rate of EnT results in a longer rise-time for the sensitized Nd(III)-based emission, which was observed to be *ca.* 200 ns [in reasonable agreement with the 256 ns decay time of the Ru(II)-based emission]. Again the Förster EnT mechanism can be ruled out: if it was not operating over 15.6 Å in RuPh·Nd it will not be operating over the greater distance in $RuPh_2$·Nd. Making the assumtion therefore that Dexter EnT is operative, as with RuPh·Nd, then the decrease in k_{EnT} associated with the additional phenylene spacer (additional length, 4.3 Å) must have an exponential distance dependence, from which it is simple to calculate an attenuation coefficient of 0.56 $Å^{-1}$. This is in

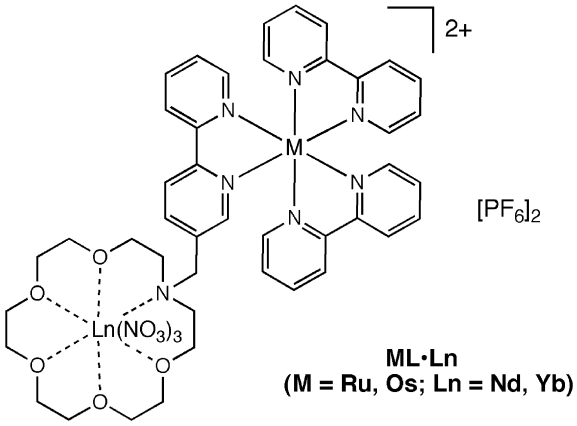

Scheme 4. The dyads ML·Ln (from Ref. [15]).

good agreement with other estimates for the electronic attenuation coefficient of *p*-phenylene spacers in systems showing long-range single electron-transfer [14], and provides additional support for the Dexter mechanism being operative for Ru → Nd EnT.

This is an interesting observation given the general and often-quoted principle that Dexter EnT is short range (because if its exponential distance dependence), and long-range EnT must occur *via* the Förster dipole–dipole mechanism with its less stringent d^{-6} distance dependence. Clearly the converse is true here, and the reason is the very low f–f absorption intensities of Ln(III) ions. This means that the Förster overlap integrals are very small as they take into account the intensity of the f–f absorptions, such that Ln(III) ions make very poor energy-acceptors when the Förster mechanism is operative. In contrast, Ln(III) ions make good Förster *donors* (as in FRET assays) because of the high intensity of the f–f emission bands, which give high J_F values when partnered with organic acceptor chromophores having fully allowed π–π^* transitions.

In contrast, since the Dexter overlap integral J_D uses *normalized* absorption spectra, the (lack of) intensity of the f–f absorptions is irrelevant and Dexter EnT can occur as long as a modest electronic coupling is present *via* the bridging ligand. So, Dexter EnT appears the only option in complexes such as $RuPh_2$·Nd in which Förster EnT is ruled out by the very low J_F value. Although a dipole/quadrupole contribution to EnT is in principle possible it is clearly not occurring given the fact that Ru → Nd EnT was diminished by a shorter but saturated bridging ligand.

2.3. Example 3: EnT by a redox-mediated mechanism in an Os(II)/Yb(III) dyad

Following the above result we examined the series of dyads shown in Scheme 4 in which both Förster and Dexter EnT should be disfavoured: the former because of the distance involved and low spectroscopic overlap integrals, and the latter because of the saturated bridge which prevents electronic coupling [15]. The complexes RuL and OsL are based on $[M(bipy)_3]^{2+}$ cores (M = Ru, Os) as energy-donors, with a pendant aza-crown macrocyclic ligand to bind the energy-accepting Ln(III) ion. In MeCN a spectroscopic titration of OsL with $Yb(NO_3)_3$ shows that the 1:1 association constant for binding of the Ln(III) in the macrocycle is *ca.* $9 \times 10^3\ M^{-1}$. Molecular mechanics calculations suggest that the metal–metal separation can lie in the range 7.4–8.4 Å because of the flexible methylene 'hinge' which allows the aza-crown macrocycle to adopt different orientations with respect to the $[M(bipy)_3]^{2+}$ core.

We performed four spectroscopic titration experiments in which small portions of $Ln(NO_3)_3$ (Ln = Yb, Nd) were added to solutions of $[M(bipy)_3](PF_6)_2$ until there was no additional change

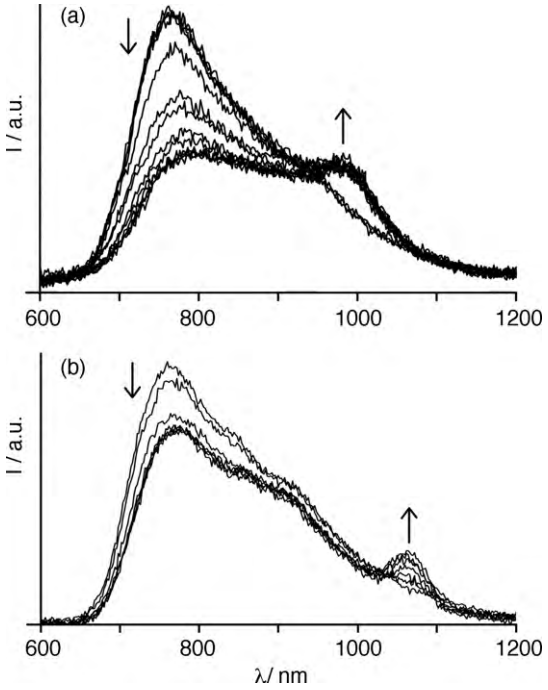

Fig. 4. Changes in luminescence spectra of OsL on titration with (a) $Yb(NO_3)_3$ hydrate and (b) $Nd(NO_3)_3$ hydrate, using MeCN as solvent. Both partial quenching of Os(II)-based emission, and the apeparance of sensitized emission from Yb(III) (at 980 nm) and Nd(III) (at 1060 nm) are evident. Fitting the intensity data at 780 nm from the sequence of spectra in (a) to a 1:1 binding isotherm afforded a binding constant of $8.9 \times 10^3\ M^{-1}$ for $Yb(NO_3)_3$ in the aza-crown macrocycle. Taken from Ref. [15].

associated with the luminescence of the Ru(II) or Os(II) centre. In both RuL·Nd and OsL·Nd, partial M → Nd EnT occurred with rate constants of 6.8×10^6 and $1.4 \times 10^7\ s^{-1}$, respectively (see Fig. 4). The numerous f–f transitions of Nd(III) in the visible region overlap with both Ru(II)-based and Os(II)-based emission spectra. The mechanism of EnT transfer here is not clear-cut. The Förster critical transfer distances are 6.0 and 5.5 Å for Ru → Nd and Os → Nd EnT, respectively: although these lie below the minimum calculated M···Ln separation of 7.4 Å the difference is not large and some Förster EnT can be expected in the most folded conformation of the complexes by both dipole–dipole and dipole–quadrupole mechanisms. (Actually the inter-chromophore separation is not the same as the metal–metal separation because the ^{3}MLCT state of the energy-donor involves both the metal centre and a bipy ligand, and is not purely metal-localised; if the ^{3}MLCT state involves the bipy ligand to which the macrocycle is attached, the actual distance over which EnT occurs is less than the metal–metal separation, which makes Förster EnT more likely). In addition a very small electronic coupling of *ca.* $0.2\ cm^{-1}$ would permit Dexter EnT to occur over this distance, and such a coupling might be possible by peripheral contact of donor and acceptor fragments. Thus small contributions from either EnT mechanism are possible.

The more interesting observation comes from comparison of RuL·Yb and OsL·Yb. The single f–f absorption of Yb(III) barely overlaps with the tail of the Ru(II)-based and Os(II)-based emission spectra so the overlap integrals J_F and J_D are much smaller than for RuL·Nd and OsL·Nd. Consequently the presence of Yb(III) caused no significant quenching of Ru(II)-based emission in RuL·Yb within the limit of sensitivity of our apparatus, indicating no significant Ru → Yb EnT by any of the Förster-type multipolar mechanisms (insufficient spectroscopic overlap) or the Dexter mechanism (insufficiently strong electronic coupling *via* the saturated linker). However, in OsL·Yb [Fig. 4(a)] the Os(II)-based luminescence is *ca.*

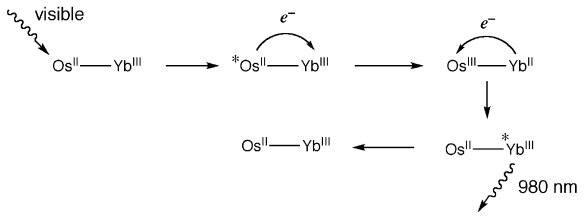

Scheme 5. Proposed mechanism for Os(II) → Yb(III) EnT in OsL·Yb, mediated *via* an initial electron-transfer step (from Ref. [15]).

50% quenched and the Os → Yb EnT rate is $2.6 \times 10^7\ s^{-1}$. This cannot involve Förster EnT, as the low J_F integral results in a critical distance of just 2.4 Å for Förster EnT; and it cannot involve Dexter EnT as this would require an unfeasibly large electronic coupling of 2 cm^{-1} to be present (if the *H* value were this large it would be equally large in the other dyads of this series and all of them would show fast Dexter EnT).

So, the Os → Yb EnT is anomalously fast and cannot be accounted for by either the Förster dipole–dipole or the Dexter mechanisms. The Förster-type dipole/quadrupole mechanism is also not likely since it does not occur to any detectable extent in RuL·Yb. However, the Horrocks redox-based mechanism is feasible in this case, as shown by the Rehm–Weller equation (Eq. (6)) [16], in which e_o is the elementary electronic charge, E_{ox} is the oxidation potential of the electron donor, E_{red} is the reduction potential of the electron acceptor, E_d is the ^{3}MLCT excited state energy of the donor group, and *w* represents the stabilisation due to a Coulombic interaction between the components of the ion pair, which varies from 0.15 eV for a closely associated ion pair in an exciplex to zero if the components are well separated.

$$\Delta G_{ET} = e_o(E_{ox} - E_{red}) - E_d - w \quad (6)$$

Cyclic voltammetric measurements show that the Os(II)/Os(III) redox couple is at +0.85 V *vs.* SCE, and the Yb(II)/Yb(III) couple is at −1.00 V *vs.* SCE. The energy available in the ^{3}MLCT state of OsL is 14,100 cm^{-1}, as determined form the position of the highest energy vibronic component of the emission spectrum of OsL at 77 K. Finally we can approximate the value of *w* in Eq. (6) (the electrostatic stabilization of the charge-separated state) as 0.1 eV. Putting these numbers into Eq. (6) equation gives a value for ΔG_{ET} – the driving force for OsL* → Yb(III) photoinduced electron-transfer, affording an Os(III)–Yb(II) charge-separated state – of *ca.* 0 eV. Given the approximations involved, especially the estimate for the value of *w*, we can say that the electron-transfer may be marginally exergonic. Importantly however, the same analysis for RuL·Yb reveals that RuL* → Yb(III) photoinduced electron-transfer is marginally less favourable, by about 0.1 eV. Although RuL has more energy available in its ^{3}MLCT state, the extra cost of oxidizing Ru(II) to Ru(III) more than offsets this and makes the excited state of $[Ru(bipy)_3]^{2+}$ a slightly less good electron donor than the excited state of $[Os(bipy)_3]^{2+}$, an observation confirmed by Lin and Sutin [17] who found that $[Os(bipy)_3]^{2+}$ is a better electron donor in the excited state than $[Ru(bipy)_3]^{2+}$ by *ca.* 120 mV. This difference in the excited state redox potentials between RuL and OsL is not large but could be just enough to tip the balance between marginally favourable OsL* → Yb(III) photoinduced electron-transfer and marginally unfavourable RuL* → Yb(III) photoinduced electron-transfer.

The sequence of events we propose is therefore shown in Scheme 5; absorption of a photon by the Os(II) centre of OsL·Yb generates the ^{3}MLCT state which performs photoinduced electron-transfer to Yb(III), generating the charge-separated Os(III)–Yb(II) state. This is only just favourable, such that the subsequent back electron-transfer step liberates close to 14,000 cm^{-1} of energy. This

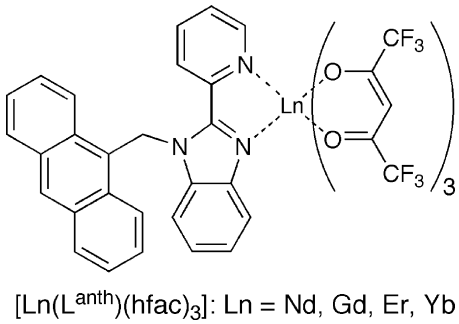

$[Ln(L^{anth})(hfac)_3]$: Ln = Nd, Gd, Er, Yb

Scheme 6. Anthracene/Ln(III) dyads based on the bridging ligand L^{anth} which contains a 2-(2-pyridyl)benzimidazole chelate coordinated to the Ln(III) with a pendant anthracenyl chromophore (from Ref. [18]).

is more than enough to pump Yb(III) into its f–f excited state (at *ca.* 10,200 cm^{-1}), resulting finally in sensitized emission from Yb(III) at 980 nm. This process is independent of the donor/acceptor spectroscopic overlap and is the only way to account for the otherwise anomalously fast Os → Yb EnT process in OsL·Yb [15].

2.4. Example 4: anthracene → Ln(III) EnT by a redox-mediated mechanism involving a diimine ligand coordinated to a Ln(III) fragment.

Our final example is not a d/f dyad but involves anthracene as an energy-donor to Nd(III), Er(III) and Pr(III). Energy-transfer from aromatic chromophores which absorb in the UV region to near-IR emissive Ln(III) ions with low-energy luminescence f–f states is well known but usually occurs *via* the conventional mechanism described in Section 1 [1] whereby the singlet π–π* state of the aromatic group (denoted ^{1}An*) is converted to the triplet state (^{3}An*) by inter-system crossing. Spectroscopic overlap with the Ln(III) ion can arise if there are high-lying f–f states whose energy is similar to that of the ^{3}π–π* state of the aromatic group, as happens commonly with Nd(III) and Er(III) for example which have numerous f–f absorptions between 10,000 and 20,000 cm^{-1}.

In our anthracene/Ln(III) dyads however we identified a new redox-based mechanism, conceptually similar to the Horrocks mechanism described above in which the first step involves photoinduced electron-transfer to Yb(III) or Eu(III) [3c], but here involving a redox-active *ligand* as intermediary rather than a redox-active lanthanide [18]. The complexes are shown in Scheme 6 and are based on a 2-(2-pyridyl)benzimidazole (denoted 'PB') chelate L^{anth}, from which an anthracenyl group is pendant, coordinated to a $\{Ln(hfac)_3\}$ fragment. A representative crystal structure is in Fig. 5. As described earlier the coordination of the N-donor chelating ligand to the $\{Ln(hfac)_3\}$ fragment is an equilibrium process (*cf.* Scheme 3), but in non-competitive solvents such as CH_2Cl_2 the binding constant is *ca.* $10^7\ M^{-1}$, such that at the considerably higher concentrations used for photophysical studies the dissociation is minimal. Examination of absorption spectra showed that the lowest absorption maximum of anthracene at 380 nm does not overlap with the absorption of the $\{Ln(hfac)_3\}$ core, such that selective excitation into the anthracene component is possible at this wavelength.

The free ligand L^{anth} shows the usual highly structured blue ^{1}An* fluorescence of anthracene with a sequence of peaks between 395 and 500 nm. As portions of $[Ln(hfac)_3(H_2O)_2]$ (Ln = Nd, Er, Yb) are added to L^{anth} and the complexes $[Ln(hfac)_3(L^{anth})]$ are formed, this fluorescence is completely quenched. We initially ascribed to inter-system crossing to give the anthracene-based ^{3}An* state which transferred its energy (*ca.* 14,500 cm^{-1}) to the Ln(III) ion in the usual way. The occurrence of sensitization of the Ln(III)-based f–f excited states was confirmed by

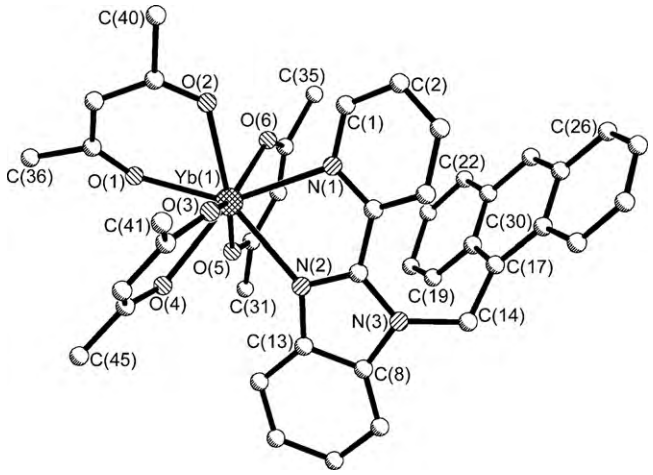

Fig. 5. Crystal structure of [Yb(hfac)$_3$(L^{anth})] with F atoms on the hfac ligands not shown for clarity (from Ref. [18]).

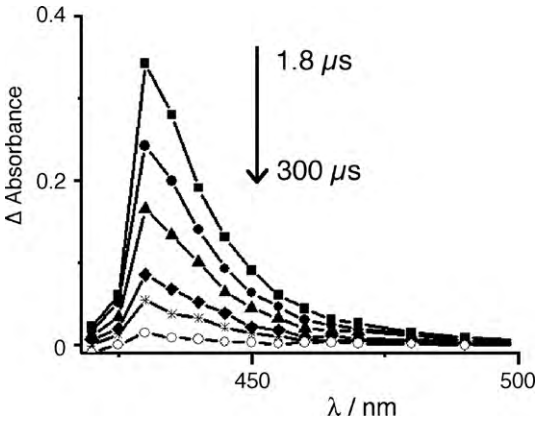

Fig. 6. Transient absorption spectrum of [Gd(hfac)$_3$(L^{anth})] in degassed toluene at RT, recorded at different time delays following 390 nm excitation pulse: 1.8, 16.2, 37, 88, 138, 300 μs (from Ref. [18]).

the observation of near-IR luminescence from the Ln(III) ions at their usual wavelengths [Yb(III), $^2F_{5/2} \rightarrow {}^2F_{7/2}$ at 980 nm; Nd(III), $^4F_{3/2} \rightarrow {}^4I_{11/2}$ and $^4F_{3/2} \rightarrow {}^4I_{11/2}$ at 1060 and 1340 nm, respectively; Er(III), $^4I_{13/2} \rightarrow {}^4I_{15/2}$ at 1530 nm] following selective excitation of the anthracene chromophore.

It was more surprising to find that an identical experiment using [Gd(hfac)$_3$(H$_2$O)$_2$] in the titration resulted in the same behaviour, with the anthracene-based ^{1}An* fluorescence being completely quenched in [Gd(hfac)$_3$(L^{anth})]. Gd(III) cannot act as an energy-acceptor as its lowest lying excited state is at *ca.* 32,000 cm^{-1}, in the UV region. The addition of Zn(II) ions and H$^+$ ions to solutions of L^{anth} likewise resulted in complete fluorescence quenching from the ^{1}An* state. These observations, together with the known redox activity of anthracene, led us to consider electron-transfer as a component of the EnT process. Anthracene undergoes oxidation and reduction processes at modest potentials. Thus, in addition to being able to participate in photoinduced energy-transfer processes, in its excited state it can also act as either an electron acceptor or an electron donor to generate the radical cation or anion, respectively [18]. Our observations are consistent with the excited anthracenyl unit acting as an electron donor in a ^{1}An* → (diimine) PET process which occurs to the coordinated PB fragment in the complexes. This is not possible in free L^{anth} in which the diimine fragment is harder to reduce so the anthracene fluorescence is not quenched by this mechanism.

The energy of the singlet excited state of the anthracene unit of L^{anth} is *ca.* 3.15 eV, estimated by averaging the energies of the lowest absorption maximum and the highest energy emission maximum. As described earlier we can use the Rehm–Weller equation (Eq. (6)) to estimate the driving force for PET, ΔG_{ET}. From the cyclic voltammogram of L^{anth} we found the anthracene unit to have an irreversible oxidation at +0.92 V *vs.* ferrocene/ferrocenium (Fc/Fc$^+$) in CH_2Cl_2. From Eq. (6) we find that the ^{1}An* unit of L^1 can act as an excited state electron donor to the PB unit as long as the PB unit reduces at a potential less negative than about −2.33 V *vs.* Fc/Fc$^+$ (taking *w* as 0.1 eV). In fact the voltammogram of free L^{anth} revealed an irreversible reduction, assumed to be PB-centred, at −2.24 V, suggesting that ^{1}An* → PB PET is marginal. Although this analysis contains significant approximations it is easy to rationalise the observed fluorescence of free L^{anth}, because the uncoordinated PB unit is not quite a sufficiently good electron acceptor to oxidise the ^{1}An* state and generate a charge-separated [An$^{\bullet+}$–(PB)$^{\bullet-}$] state by PET. When a Ln(III) ion [or a Zn(II) ion, or a proton] is coordinated to the PB unit in the complexes however the PB fragment becomes reduced much more easily, and E_{red} in Eq. (6) becomes less negative; coordinated PB ligands typically have reduction potentials that are about 400–500 mV less negative than the free ligand [19]. Similar behaviour is seen with related bipyridine ligands: for example free 2,2′-bipyridine undergoes an irreversible reduction at −1.86 V *vs.* NHE, which shifts to −1.26 V *vs.* NHE in [Ru(bipy)$_3$]$^{2+}$ [20].

So, we know that (i) a PET step to give a charge-separated {An$^{\bullet+}$–(PB$^{\bullet-}$)Ln} state occurs after excitation of the anthracene chromophore, and (ii) collapse of this somehow generates the emissive f–f states of Nd(III), Er(III) and Yb(III). The question then arises: does back ET from the charge-separated state generate the f–f excited state of the lanthanide directly (as in the Horrocks mechanism when a lanthanide has been transiently reduced to the +2 state [3c]), or does it first generate the ^{3}An* state (energy content 1.8 eV) which then donates its energy to the Ln(III) centre in a subsequent step? The presence of the ^{3}An* state as an intermediate was confirmed by transient absorption spectroscopy measurements on [Gd(hfac)$_3$(L^{anth})] and [Nd(hfac)$_3$(L^{anth})] in deoxygenated toluene solutions at room temperature using selective excitation into the lowest energy absorption feature of the anthracene unit at 390 nm. After excitation both complexes show a transient absorption feature at 430 nm which is characteristic of the ^{3}An* absorbance (Figs. 6 and 7). No rise-time for this absorbance was detected, which means that it must appear in <20 ns, the limit of our equipment. In [Gd(hfac)$_3$(L^{anth})] this ^{3}An* state was long lived (≈70 μs), but in [Nd(hfac)$_3$(L^{anth})] it was rapidly quenched with a lifetime of just 130 (±20) ns implying that that the ^{3}An* state is acting as

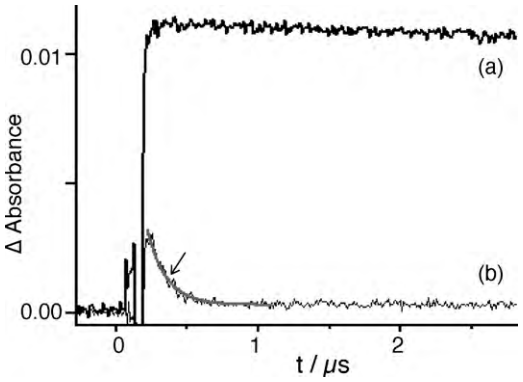

Fig. 7. Decay kinetics of ^{3}An* recorded at 430 nm in degassed toluene at RT under 390 nm excitation, for (a) [Gd(hfac)$_3$(L^{anth})] and (b) [Nd(hfac)$_3$(L^{anth})]. The gray line on (b) (indicated with an arrow) represents a monoexponential fit to the decay of the transient absorption, with the lifetime 130 (±20) ns. Instrument response *ca.* 20 ns.

the energy-donor to Nd(III). Conformation of this was provided by time-resolved measurements on the sensitized Nd(III) emission band at 1060 nm, which showed a rise-time of 130 ns before the usual decay of *ca.* 1 μs; this good match between the decay of the ^{3}An* state and the grow-in of the Nd(III) sensitized luminescence clearly shows that they are linked.

We note that this relatively slow energy-transfer rate ($<10^7$ s^{-1}) is entirely consistent with a conventional Förster or Dexter energy-transfer mechanism to Nd(III) which is slow because of a combination of an electronically saturated pathway (*i.e.* no conjugated linkage) between donor and acceptor, and poor donor/acceptor spectroscopic overlap. In contrast an energy-transfer rate this slow would be difficult to rationalize if it arose from a back ET step [An$^{\bullet+}$–(PB$^{\bullet-}$)Ln] → [An–(PB)Ln*] without the intermediacy of the ^{3}An* state, as this would imply the existence of a charge-separated state with a remarkably long lifetime of 130 ns.

The anthracene → Ln(III) PEnT mechanism in these complexes is summarized by the following sequence of steps: [^{1}An*–(PB)Ln] → [An$^{\bullet+}$–(PB$^{\bullet-}$)Ln] → [^{3}An*–(PB)Ln] → [An–(PB)Ln*]. The occurrence of the first electron-transfer step to generate the charge-separated state [An$^{\bullet+}$–(PB$^{\bullet-}$)Ln] is made possible by the strong stabilisation of the LUMO of the PB fragment of L^{anth} on coordination to a {Ln(hfac)$_3$} unit. This charge-separated state was too short lived to be detected using our transient absorption equipment and quickly performs back ET to generate [^{3}An*–(PB)Ln] which acts as the ultimate energy-donor to the Ln(III) centre in the usual way. This mechanism bears obvious similarities to the Horrocks mechanism which involves photoinduced electron-transfer from a sensitizer to Eu(III) or Yb(III) [3c], but is more general in that it involves the coordinated diimine ligand so is independent of the nature of the lanthanide ion.

3. Conclusions

In this series of studies we have clarified the mechanisms contributing to d–f energy-transfer in three different sets of dyads, and have also found an unusual redox-based mechanism for energy-transfer in a series of anthracene/Ln(III) dyads.

Acknowledgements

The author gratefully thanks his coworkers and collaborators who are named in the reference list: in particular Prof. Stephen Faulkner (Universities of Manchester and Oxford) and Dr. Andrea Barbieri (Istituto-ISOF, Bologna) have made this work possible by their photophysical measurements and calculations.

References

[1] (a) S. Lis, M. Elbanowski, B. Makowska, Z. Hnatejko, J. Photochem. Photobiol. A: Chem. 150 (2002) 233;
(b) N. Sabbatini, M. Guardigli, J.-M. Lehn, Coord. Chem. Rev. 123 (1993) 201;
(c) G.F. De Sa, O.L. Malta, C. de Mello Donega, A.M. Simas, R.L. Longo, P.A. Santa-Cruz, E.F. da Silva Jr., Coord. Chem. Rev. 196 (2000) 165;
(d) S. Faulkner, J.L. Matthews, in: M.D. Ward (Ed.), Comprehensive Coordination Chemistry, vol. 9, 2nd ed., Elsevier, 2004, p. 913;
(e) S. Sato, M. Wada, Bull. Chem. Soc. Jpn. 43 (1970) 1955;
(f) D. Parker, J.A.G. Williams, J. Chem. Soc., Dalton Trans. (1996) 3613.
[2] G.A. Hebbink, S.I. Klink, L. Grave, P.G.B.O. Alink, F.C.J.M. van Veggel, Chem. Phys. Chem. 3 (2002) 1014.
[3] (a) S. Faulkner, B.P. Burton-Pye, T. Khan, L.R. Martin, S.D. Wray, P.J. Skabara, Chem. Commun. (2002) 1668;
(b) A. Beeby, S. Faulkner, J.A.G. Williams, J. Chem. Soc., Dalton Trans. (2002) 1918;
(c) W.D. Horrocks Jr., J.P. Bolender, W.D. Smith, R.M. Supkowski, J. Am. Chem. Soc. 119 (1997) 5972.
[4] (a) M.D. Ward, Coord. Chem. Rev. 251 (2007) 1663;
(b) S. Faulkner, L.S. Natrajan, W.S. Perry, D. Sykes, Dalton Trans. (2009) 3890.
[5] D.L. Dexter, J. Chem. Phys. 21 (1953) 836.
[6] Th. Förster, Discuss. Faraday Soc. 27 (1959) 7.
[7] (a) C.A. Royer, Chem. Rev. 106 (2006) 1769;
(b) P.R. Selvin, Ann. Rev. Biophys. Biomol. Struct. 31 (2002) 275;
(c) P.R. Selvin, Nature Struct. Biol. 7 (2000) 730.
[8] G.D. Scholes, Annu. Rep. Phys. Chem. 54 (2003) 57.
[9] (a) P.P. Lima, S.S. Nobre, R.O. Freire, S.A. Júnior, R.A. Sá Ferreira, U. Pischel, P.L. Malta, L.D. Carlos, J. Phys. Chem. C 111 (2007) 17627;
(b) J.O. Rubio, A.F. Muñoz, G.H. Muñoz, M.E. López-Morales, J. Phys. C: Solid State Phys. 21 (1988) 2059;
(c) O.L. Malta, J. Lumin. 71 (1997) 229.
[10] (a) G.M. Davies, S.J.A. Pope, H. Adams, S. Faulkner, M.D. Ward, Inorg. Chem. 44 (2005) 4656;
(b) J.-M. Herrera, S.J.A. Pope, H. Adams, S. Faulkner, M.D. Ward, Inorg. Chem. 45 (2006) 3895;
(c) J.-M. Herrera, S.J.A. Pope, A.J.H.M. Meijer, T.L. Easun, H. Adams, W.Z. Alsindi, X.-Z. Sun, M.W. George, S. Faulkner, M.D. Ward, J. Am. Chem. Soc. 129 (2007) 11491;
(d) S.G. Baca, S.J.A. Pope, H. Adams, M.D. Ward, Inorg. Chem. 47 (2008) 3736.
[11] T. Lazarides, G.M. Davies, H. Adams, C. Sabatini, F. Barigelletti, A. Barbieri, S.J.A. Pope, S. Faulkner, M.D. Ward, Photochem. Photobiol. Sci. 6 (2007) 1152.
[12] H. Kunkely, A. Vogler, Inorg. Chem. Commun. 7 (2004) 770.
[13] T. Lazarides, D. Sykes, S. Faulkner, A. Barbieri, M.D. Ward, Chem. Eur. J. 14 (2008) 9389.
[14] (a) F. Barigelletti, L. Flamigni, Chem. Soc. Rev. 29 (2000) 1;
(b) B. Schlicke, P. Belser, L. De Cola, E. Sabbioni, V. Balzani, J. Am. Chem. Soc. 121 (1999) 4207;
(c) F. Barigelletti, L. Flamigni, M. Guardigli, A. Juris, M. Beley, S. Chodorowski-Kimmes, J.-P. Collin, J.-P. Sauvage, Inorg. Chem. 35 (1996) 136.
[15] T. Lazarides, N.M. Tart, D. Sykes, S. Faulkner, A. Barbieri, M.D. Ward, Dalton Trans. (2009) 3971.
[16] D. Rehm, A. Weller, Isr. J. Chem. 8 (1970) 259.
[17] C.-T. Lin, N. Sutin, J. Phys. Chem. 80 (1976) 97.
[18] T. Lazarides, M.A.H. Alamiry, H. Adams, S.J.A. Pope, S. Faulkner, J.A. Weinstein, M.D. Ward, Dalton Trans. (2007) 1484.
[19] N.M. Shavaleev, Z.R. Bell, T.L. Easun, R. Rutkaite, L. Swanson, M.D. Ward, Dalton Trans. (2004) 3678.
[20] (a) P. Belser, A. von, Zelewsky, Helv. Chim. Acta 63 (1980) 1675;
(b) A. Juris, V. Balzani, F. Barigelletti, S. Campagna, P. Belser, A. von Zelewsky, Coord. Chem. Rev. 84 (1988) 85.